ACS APPLIED MATERIALS & INTERFACES

Research Article

www.acsami.org

Triangular Platinum(II) Metallacycles: Syntheses, Photophysics, and Nonlinear Optics

Yuanpeng Fan and Dahui Zhao*

Beijing National Laboratory for Molecular Sciences, Department of Applied Chemistry, Center for Soft Matter Science and Engineering, the Key Laboratory of Polymer Chemistry and Physics of the Ministry of Education, College of Chemistry, Peking University, Beijing 100871, China

Supporting Information

ABSTRACT: Three triangular platinum(II) diimine metallacycles incorporating large cyclic oligo(phenylene-ethynylene) (OPE) bisacetylide ligands are synthesized, and their photophysical properties are studied. Two types of triplet excited states with ligand/metal-to-ligand charge-transfer and acetylide-ligand-centered characteristics respectively, are exhibited by these complexes depending on the size (conjugation length) and electronic features of the cyclic OPE ligands. When the energy levels of the two excited states are close to each other, the lowest triplet state is found to switch between the two in varied solvents, resulting from their relative energy inversion induced by solvent polarity change. Density functional theory and time-dependent density functional theory calculations provide corroborative evidence for such experimental conclusions. More importantly, the designed metallacycles show impressive two-photon absorption (2PA) and two-photon excitation phosphorescing abilities, and the 2PA cross section reaches 1020 GM at 680 nm and 670 GM at 1040 nm by two different metallacycles. Additionally, pronounced reverse saturable absorptions are observed with these metallacycles by virtue of their strong transient triplet-state absorptions.

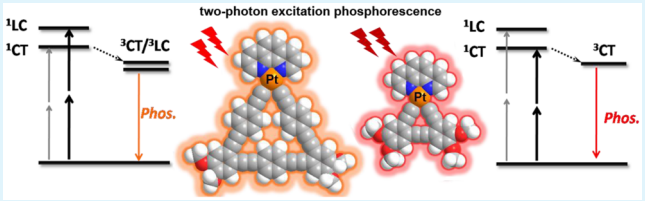

KEYWORDS: *platinum(II) acetylide, platinum metallacycle, two-photon absorption, reverse saturable absorption, nonlinear optics*

INTRODUCTION

Pt(II) acetylide complexes are emerging functional materials with innovative uses in light emitting,[1,2] photovoltaics,[3] bioimaging,[4] chemosensing,[5,6] energy upconversion,[7,8] and so on. All these applications harness the optimal optoelectronic properties of the readily accessible triplet states of the complexes, as well as their unique supramolecular behaviors related to the square-planar coordination geometry.[9−12] On the other hand, with the vast advancement of laser technology, nonlinear optical (NLO) materials, for example two-photon absorption (2PA) systems, demonstrate versatile functions in a range of technologies including optical data storage, optical limiting, microfabrication, optical imaging, and so on.[13−17] Combining the above two appealing aspects of characters, Pt(II) complexes manifesting NLO properties are of great theoretical and practical values.[18,19]

Some previous investigations show that, similar to organic molecules, large planar conjugated scaffolds and electron push−pull features are favorable factors for attaining optimal NLO properties in metal complexes.[20−22] A number of *trans*-Pt bisacetylide complexes having phosphine ligands were systematically studied and demonstrated impressive NLO activities in the visible to near-infrared regime.[23−27] Particularly, when the complexes were installed with polarizable electron donor and acceptor groups, the 2PA abilities are greatly enhanced. On the other hand, when bidentate diimine ligands are incorporated, Pt bisacetylides of *cis*- configuration were realized, exhibiting rich and interesting linear and nonlinear photophysical behaviors, which could be sensitively tuned by modifying the acetylide ligand structures.[28−41] A range of appealing properties were displayed and investigated, such as triplet excited-state absorptions[31−38] and triplet sensitizing abilities[39−41].

In addition to tailoring the electronic properties, we speculate that introducing cyclic topology may be an effective approach to improving and tuning the NLO properties of metal complexes. This tactic was proven successful with a number of organic 2PA molecules.[42−44] Nonetheless, although various Pt(II) metallacycles have been reported in the literature, demonstrating interesting supramolecular chemistry such as self-assembly ability and host−guest interactions,[34,45−49] the NLO properties of pertinent structures are basically unexplored.

Here we prepare and study a series of Pt(II) metallacycles featuring cyclic oligo(phenylene-ethynylene) (OPE) ligands of different sizes and electronic characteristics. Their photophysical properties are investigated, with special attention paid to the 2PA and excited-state absorption attributes. All herein synthesized Pt(II) metallacycles (**C1**−**C3**) comprise a diimine-type ligand of 1,10-phenathroline. To achieve the cyclic framework, three different OPE structures (**L1**−**L3**) are

Received: December 23, 2014
Accepted: March 4, 2015
Published: March 4, 2015

© 2015 American Chemical Society

DOI: 10.1021/am509074m
ACS Appl. Mater. Interfaces 2015, 7, 6162−6171

designed and employed to construct the triangular metallacycle skeletons by coordinating to Pt(II) via two terminal acetylene groups. For comparison, we also examined an acyclic analogue complex **4** bearing two acyclic OPE ligands. In general, our study shows that **C1**−**C3** exhibit considerably enlarged 2PA cross sections compared to the acyclic analogue **4**, and pronounced excited-state absorptions are detected. The results demonstrate that the Pt OPE metallacycles possess rich and interesting triplet-state and NLO properties, which are sensitively dependent on the size and electronic features of the cyclic bisacetylide ligands.

RESULTS AND DISCUSSION

Syntheses and Characterizations. Among the three designed triangular metallacycles, **C1** and **C2** are both attached with four alkoxy side chains to the *o*-phenylene units in the OPE ligands. **C1** contains a larger cyclic ligand than **C2** because it incorporates three additional *p*-phenylene-ethynylene units. The cyclic bisacetylide ligand in metallacycle **C3** has an identical chain length to that of **C1**, but two alkyl side chains are connected to the OPE backbone via the phthalimide functional groups. Complex **4** lacks the cyclic topology and incorporates two linear OPE ligands, each tethered with an alkoxy group at the OPE chain end. The four OPE ligands, **L1**−**L4**, are prepared using previously established procedures involving stepwise OPE chain extension strategy (see the Supporting Information for details).[50] Complexes **C1**−**C3** are synthesized by subjecting **L1**−**L3** to dichloro(1,10-phenanthroline)platinum(II) (Pt(phen)Cl_2) under typical conditions for acquiring Pt acetylides reported in the literature.[34] The only difference is that more dilute reaction solutions are used to facilitate the intramolecular cyclizations and achieve the cyclic scaffolds (Scheme 1). The chemical structures of all four complexes (**C1**−**C3** and **4**) are characterized and confirmed by ^{1}H and ^{13}C NMR spectra, as well as mass spectroscopy.

Scheme 1. Syntheses of C1−C3 and 4

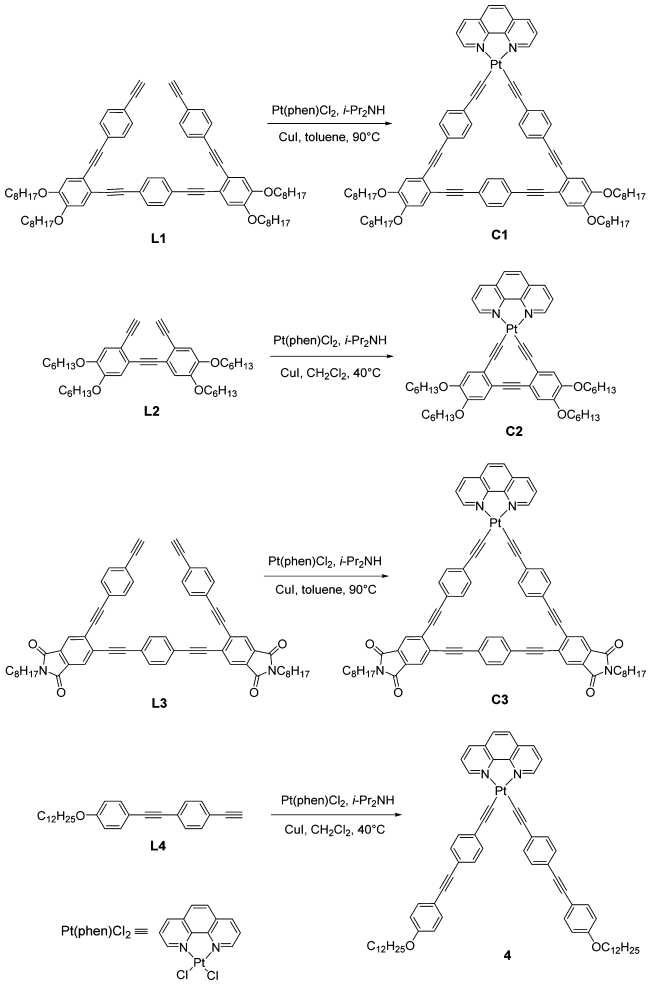

Ground-State Linear Absorptions and Emissions. The linear photophysical properties of Pt complexes **C1**−**C3** and **4** are first examined in toluene solution. All four molecules show major absorption bands in the UV region of 300−400 nm (Figure 1a and Table 1). These dominant peaks are assigned to the OPE ligand-based transitions, as similar band shapes and extinction coefficients are displayed by respective ligands **L1**−**L4** (Figure S1, Supporting Information). Consistent with previously reported Pt(II) acetylide systems,[20,21,25] the bathochromic shifts displayed by the complexes relative to the ligands are attributed to the delocalization of ligand-based π/π^* molecular orbitals (MO) via interactions with Pt dπ orbitals.

In addition to the ligand-based main transitions, the complexes also show relatively broad absorption tails reaching into the visible region of more than 400 nm. Similar to other Pt(II) diimine acetylides,[1,5,28,29] these lower-energy absorption bands should originate from metal-to-ligand and ligand-to-ligand charge transfer (MLCT/LLCT) transitions. Such assignments are also supported by the density functional theory (DFT) and time-dependent DFT (TD-DFT) calculations (vide infra). Relative to the acyclic analogue **4**, also bearing alkoxy groups on the OPE ligands, metallacycle **C1** exhibits a small bathochromic shift in these CT transitions, which reflects a minor enhancement of the electron-donating effect of the cyclic OPE ligand, presumably due to the larger π-conjugation system. On the other hand, complex **C2** has a smaller cyclic OPE skeleton and displays a significantly red-shifted and more pronounced CT band around 520 nm. We deem that this property likely results from the shorter π-bridge between Pt(phen) moiety and the electron-rich dialkoxyphenylene units in **C2**, which entails a stronger CT effect between the charge donor (Pt-acetylide) and acceptor (phenanthroline). This assumption is corroborated by the DFT calculation results, revealing a much higher highest occupied molecular orbital (HOMO) of **C2** than those of **C1** and **4** (Figure S9, Supporting Information). On the other hand, when we compare **C1** and **C3** having OPE ligands of the same length, the CT absorption band is slightly blue-shifted when the alkoxy side groups are replaced by the *N*-alkyl phthalimide functionality. This observation is ascribed to the electron-withdrawing effect of the phthalimide group, which lowers the electron density on the OPE ligand in **C3** and thus enlarges the energy gap of the LLCT/MLCT transitions.

Furthermore, when the absorption spectra are collected in a series of different solvents, all studied Pt(II) complexes demonstrate a negative solvatochromic effect in their CT absorption bands (Figure S2, Supporting Information), while the ligand-based main transitions are nearly solvent independent. Such phenomena indicate that in these complexes, the vertically accessed CT excited states are less polar than their respective ground states. Similar behaviors were also observed with a number of other Pt(II) acetylide systems.[1,28,30,34,37,51−53] Among the current four complexes, **C2** manifests the most

DOI: 10.1021/am509074m
ACS Appl. Mater. Interfaces 2015, 7, 6162−6171

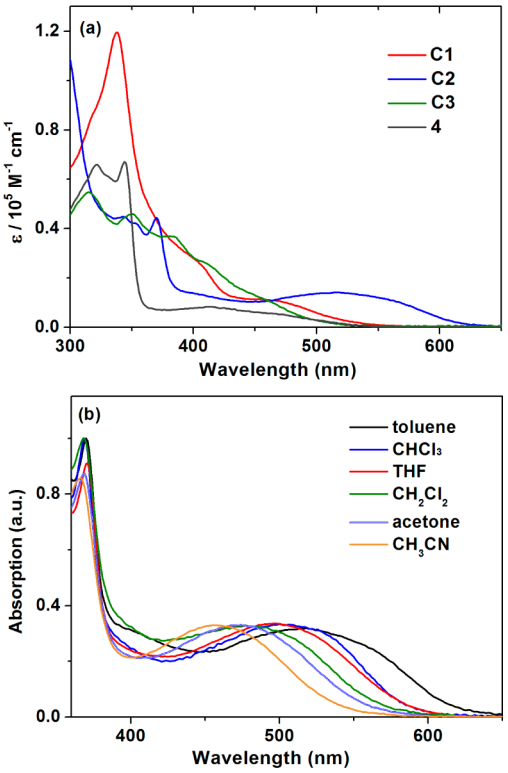

Figure 1. (a) Ground-state absorption spectra of **C1**−**C3** and **4** in toluene at 10 μM; (b) absorption spectra of **C2** in different solvents.

evident hypsochromic shifting in its CT band with increasing solvent polarity (Figure 1b).

The photoluminescence properties are subsequently examined. Under ambient conditions, two distinct emission bands are detected for each complex in toluene solution (Figure S3, Supporting Information). The peaks of higher energy are fluorescence emissions, which are of nanosecond lifetimes, insensitive to oxygen, and similarly shown at about 420 nm by all four complexes. The lower-energy peaks are identified as phosphorescence emissions originating from the triplet excited states, in light of their sensitivity to oxygen quenching and microsecond lifetimes under deoxygenated conditions.

Specifically, acyclic complex **4** exhibits a broad, featureless emission band around 590 nm at room temperature (Figure 2a), which is found to undergo significant hypsochromic

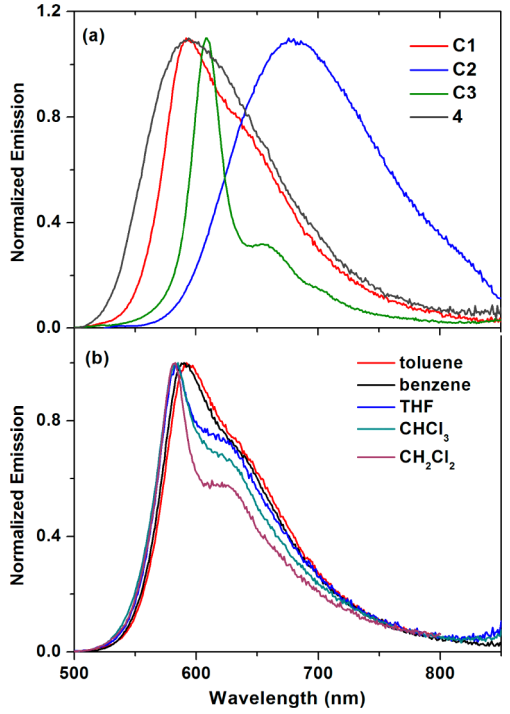

Figure 2. Normalized phosphorescence spectra of (a) **C1**−**C3** and **4** in toluene and (b) **C1** in different solvents at room temperature (excited at respective absorption maxima with O.D. = 0.1 under deoxygenated conditions).

shifting upon freezing at 77 K (Figure S4, Supporting Information). Such emission properties indicate the dominant ^{3}CT characteristics of the lowest triplet state (T_1) in **4**.[28,34] Such an assignment is also in agreement with the relatively short emission lifetime of **4** (Table 1). In comparison, perceptibly different T_1 properties are observed with metallacycle **C1**. While a relatively short phosphorescence lifetime of 2.4 μs and fairly rapid radiative decay at $>10^5$ s^{-1} still emphasize the main CT features of the T_1 state at room temperature,

Table 1. Absorption and Phosphorescence Properties[a]

	absorption	phosphorescence[b]					2PA cross sections[c]	
	λ_{abs}/nm (ε/10^4 M^{-1}cm^{-1})	λ_{em}/nm	τ/μs[d]	Φ_p[e]	k_r/10^5 s^{-1}	k_{nr}/10^5 s^{-1}	λ_{2PA}/nm	σ/GM
C1	338 (12)	592 (576)	2.4 (195)	0.25	1.1	3.4	680 (680)	1020 (1060)
	408 (2.5)						860 (840)	260 (280)
	458 (1.1)							
C2	370 (4.4)	675 (599)	0.13 (13)	0.018	1.4	76	740 (740)	120 (95)
	518 (1.4)						1040 (940)	670 (710)
C3	315 (5.5)	608 (603)	56 (150)	0.056	0.01	0.17	700 (700)	610 (620)
	350 (4.6)							
	381 (3.7)							
4	321 (6.7)	594 (530)	1.1 (14)	0.25	2.3	6.9	680 (680)	40 (36)
	344 (6.8)						860 (820)	17 (19)
	414 (0.8)							

[a]Absorption and emission data are measured in deoxygenated toluene solution at 298 K unless otherwise noted. [b]Data in parentheses are collected at 77 K in 2-MeTHF. [c]Data in parentheses are measured in CH_2Cl_2. [d]Phosphorescence lifetimes of <20 μs are measured by time-correlated single-photon counting using NanoLED of 450 or 495 nm as excitation source; longer lifetimes (>20 μs) are determined with a pulsed Xe lamp. [e]Phosphorescence quantum yields Φ_p are determined with $Ru(bpy)_3Cl_2$ (Φ_p = 0.062 in deoxygenated CH_3CN) as the reference.

DOI: 10.1021/am509074m
ACS Appl. Mater. Interfaces 2015, 7, 6162−6171

metallacycle **C1** displays a slightly narrowed phosphorescence band compared to that of **4**, with noticeable vibronic features (Figure 2a). Moreover, although nearly identical phosphorescence quantum yields ($\Phi_p \approx 0.25$) are detected for **C1** and **4**, a roughly doubled excited-state lifetime is observed with the cyclic complex, resulting from both smaller radiative (k_r) and nonradiative (k_{nr}) decay rates. All these spectral properties suggest that although the T_1-S_0 relaxation in **C1** mainly demonstrates ^{3}LLCT/MLCT properties, it is evidently disturbed by ligand-centered (LC) processes, which typically slow down the triplet state relaxation due to less heavy-atom effect. Apparently, the extended emission lifetime of **C1** is also related to the higher rigidity of its cyclic OPE ligand. Moreover, at 77 K, a much smaller hypsochromic shift is manifested by **C1** than by **4**. This is also consistent with the admixing of LC component in the T_1 relaxation of **C1**, because the LC transition energies are typically less sensitive to temperature due to the minimal reorganization.[28,54,55]

In contrast, when the side groups are altered from alkoxy to dicarboximide, metallacycle **C3** exhibits a much narrower phosphorescence band, showing clearly resolved vibronic structures and a drastically extended lifetime of >50 μs at room temperature (Table 1). Moreover, very similar emission maxima and band shape are displayed at various temperatures (Figure S4, Supporting Information). These properties unambiguously indicate that the T_1-S_0 transition of **C3** is dominated by a ^{3}LC process. A considerably smaller Φ_p (~0.06) is observed with **C3** than that of **C1**, resulting from its drastically decreased k_r, by approximately 2 orders of magnitude, whereas its k_{nr} is reduced to a much smaller extent.

Notably, compared to those of **C1** and **4**, the triplet emission of **C2** is significantly red-shifted to nearly 680 nm in toluene, in line with its much lower energy of the CT absorption band. The particularly short emission lifetime (~0.1 μs) and large hypsochromic shifting at 77 K are both indicative of a ^{3}CT-governed T_1 relaxation in this metallacycle. A small Φ_p value (<2%) is also detected with **C2**, but for a different reason than **C3**. Such a low emission efficiency is mainly resultant from substantially enlarged k_{nr} of nearly 8×10^6 s^{-1} (Table 1). Such a k_{nr} upsurge is in accordance to the band gap law and the more pronounced CT characteristic of **C2**. In summary of triplet-state properties in toluene solution, the experimental results indicate that, while the T_1-S_0 transitions in **C2** and **4** are dominated by ^{3}CT processes,[1,28] **C1** features a LC-disturbed ^{3}CT transition, and a ^{3}LC-dominated relaxation occurs to **C3**.[54,55] Such propositions are generally confirmed by subsequent theoretical calculations.

When the emission properties are examined in alternative solvents, a minor negative solvatochromic effect is exhibited by **C1**. More importantly, perceptible changes are observed with the band shape. Specifically, as the solvent is changed from benzene or toluene to CH_2Cl_2, in addition to a hypsochromic shift, the emission band becomes increasingly narrowed, manifesting more and more pronounced vibronic features (Figure 2b). Additionally, time-resolved experiments show that in toluene and benzene **C1** exhibits a short triplet lifetime of ca. 2.4 μs, with k_r and k_{nr} both at the order of 10^5 s^{-1}. When the solvent is switched to CH_2Cl_2, the emission lifetime is prolonged to over 10 μs at room temperature (Table S1, Supporting Information). With k_r curbed to a greater extent than k_{nr}, Φ_p of **C1** diminishes from 0.25 in toluene to 0.10 in CH_2Cl_2. All these behaviors suggest that **C1** experiences a T_1 property alteration in response to the solvent variation. Namely, unlike the ^{3}LLCT/MLCT transition disturbed by ^{3}LC process observed in nonpolar solvents, a ^{3}LC-dominated T_1 relaxation emerges in more polar solvents such as CH_2Cl_2, although it is likely mixed with certain CT component. Similar phenomena of T_1 inversion were reported previously with a couple of other Pt acetylide complexes.[28,29] In general, this lowest excited-state switching may occur when the ^{3}CT and ^{3}LC transitions are very close in energy. When the ^{3}CT excited state is less polar than the ground state, resulting from a reversed charge transfer direction (cf. theoretical calculations for **C1**), a larger energy gap is produced in high-polarity solvents. On the other hand, the energy gap of ^{3}LC transition is usually less sensitively influenced by solvent polarity, due to the smaller polarity difference between the excited and ground states. Thus, the ^{3}LLCT/MLCT transition of **C1** is of lower energy than ^{3}LC transition in less polar solvents but becomes higher in energy in the solvents of higher polarity.

Such a T_1 switching phenomenon is not exhibited by the other three studied complexes; similar phosphorescing properties are displayed in different solvents by these complexes (Figure S5 and Tables S2–S4, Supporting Information). Unlike its absorption spectrum showing a negative solvatochromic effect, a positive solvatochromic process is detected with the emission of **C2**, implying that its T_1 state is slightly more polar than its ground state, although the vertically reached triplet excited state via absorption has a lower polarity. Nonetheless, the emission band shape remains unchanged in various solvents for **C2**, suggesting a consistent ^{3}CT transition under different solvent conditions. Meanwhile, **C3** also exhibits nearly invariable phosphorescence band shape and wavelengths in different solvents, suggesting similar polarity of its T_1 and S_0 states, as well as an unvarying ^{3}LC-dominated transition. For acyclic complex **4**, nearly identical emission spectra are exhibited in varied solvents, indicating similar ^{3}CT-featured relaxations (Figure S5, Supporting Information).

Computational Studies. To further understand the photophysical properties, DFT and TD-DFT calculations are conducted at the PBE1PBE/SDD (6-31G(d,p)) level.[56] First, the geometry optimizations are performed for the closed-shell structures. In the three metallacycles, the cyclic OPE backbones are generally coplanar with the Pt(phen) moiety, except that the *p*-phenylene units are slightly tilted out of the plane in **C1** and **C3**. For acyclic complex **4**, the two acetylide ligands are however pointed out of the plane of Pt(phen) (Figure S6, Supporting Information). For all four complexes, the HOMOs are delocalized over platinum and OPE ligand backbones. While the lowest unoccupied molecular orbitals (LUMOs) of **C1**, **C2**, and **4** are completely located with Pt(phen), the LUMO in **C3** is suggested to distribute over both phen and part of OPE (Figure 3).

In general, the TD-DFT calculations (Tables S5–S13, Supporting Information) offer agreeable results to the conclusions drawn from the spectral data. While the higher-energy absorption peaks of the complexes are confirmed related to OPE ligand-based $\pi-\pi^*$ transitions, the lower-energy bands are assignable to the LLCT/MLCT processes. Moreover, all four complexes show relatively large permanent dipole moments in the ground state (10–24 D), pointing from Pt(phen) to OPE ligands. In both polar and nonpolar solvents, **C2** and **4** are shown to exhibit reversed dipoles in their excited states, consistent with their LLCT/MLCT nature (with phenanthroline acting as charge acceptor). In contrast, while a reversed dipole is calculated for the excited state of **C1** in

DOI: 10.1021/am509074m
ACS Appl. Mater. Interfaces 2015, 7, 6162–6171

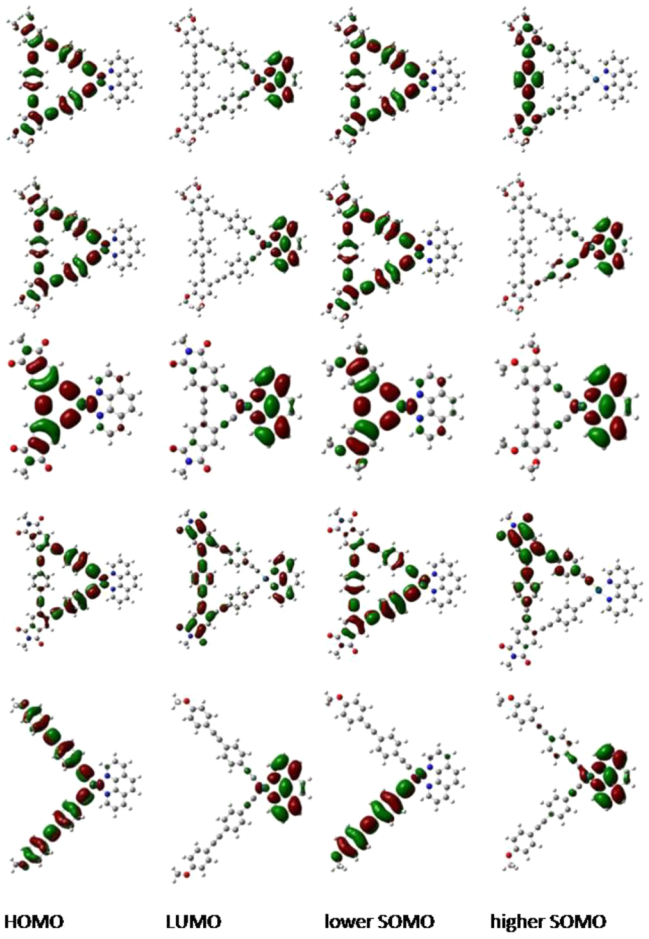

Figure 3. Calculated molecular orbitals of complexes (top to bottom) **C1** in CH_2Cl_2 and **C1**, **C2**, **C3**, and **4** in toluene.

toluene, in accordance to a ^{3}CT excited state, this metallacycle is predicted to retain its dipole moment in the same direction with a similar magnitude upon excitation in CH_2Cl_2. This result supports a ^{3}LC-featured excited state of **C1** in polar solvents (Table S14, Supporting Information). Basically, the calculation results substantiate the experimental conclusion in that the excited state of **C1** manifests a solvent-dependent identity, which switches between ^{3}CT and ^{3}LC transitions depending on the medium polarity. Regardless of the solvent, the dipole moment in **C3** nonetheless maintains the same orientation in the ground and excited states, also proving that **C3** possesses a ^{3}LC relaxation of T_1.

Geometry optimizations and calculations are also conducted for the lowest triplet states using unrestricted formalism. The calculated singly occupied molecular orbitals (SOMOs) further confirm that in both toluene and CH_2Cl_2 **C2** and **4** depict mainly ^{3}LLCT/MLCT-featured transitions, while **C3** exhibits a ^{3}LC-dominated transition restricted to the OPE ligand (Figure 3 and Figure S16, Supporting Information). More importantly, calculated SOMOs further verify that ^{3}LLCT/MLCT and ^{3}LC-dominated transitions take place with **C1** in toluene and CH_2Cl_2, respectively. Specifically, while HOMO and the lower SOMO are similarly located with Pt and OPE ligand in both solvents, the higher SOMO is mostly found with phenanthroline in toluene, with minor contributions from OPE, but it is completely shifted to a segment of OPE ligand in CH_2Cl_2 (Figure 3).

Two-Photon Absorption and Two-Photon Excitation Phosphorescence. Compared with previously reported Pt bisacetylide complexes which exhibit prominent 2PA abilities,[20−27,57,58] the unique feature of currently investigated complexes lies in their cyclic topology. Here, the 2PA properties are examined by monitoring the two-photon excitation phosphorescence. To ensure that intrinsic 2PA cross sections (σ) are properly determined, a femtosecond laser with a low repetition frequency of 1 kHz is employed as the excitation source. Yellow to red phosphorescence emissions are detected from the complexes in toluene solutions upon excitation at 800 nm (Figure S17, Supporting Information). Because none of the complexes displays linear absorptions beyond 700 nm, the detected emissions are reasonably attributed to nonlinear excitation processes. The two-photon excitation mechanism is further verified by the linear dependence of phosphorescence intensity on the square of the incident laser power (Figure S18, Supporting Information). Subsequently, 2PA cross sections at varied wavelengths are determined for each complex using the comparative method, that is, by measuring the phosphorescence intensity and calibrating it relatively to the emission from Rhodamine B as a reference.[59]

In general, the four complexes show evident 2PA activities in a relatively broad spectral range from far-red to near-infrared (NIR) region (Figure 4). Specifically, the two-photon excitation spectra of **C1** and **4** well match double the wavelengths of their respective 1PA spectra (i.e., $\lambda_{2PA} \approx 2\lambda_{1PA}$) which is a plausible result considering their noncentrosymmetric structures.[2,30,57] Remarkably, while acyclic **4** demonstrates a 2PA σ maximum of merely 40 GM at about 680 nm, metallacycle **C1** exhibits a 2PA σ maximum of over 1×10^3 GM at a similar wavelength (Table 1). Additionally, **C1** also manifests perceivable 2PA activity in the NIR regime, and a cross section of 260 GM is determined at 860 nm as a local maximum. These results clearly confirm that by constructing a metallacycle structure, the 2PA ability can be dramatically improved with relevant Pt complexes. The more extended and polarizable π-conjugated scaffold and more planar conformation of the OPE ligand both contribute to the enlargement of 2PA cross sections. Notably, compared with 1PA spectra, the 2PA sideband appearing at >800 nm in both **C1** and **4** is slightly enhanced relatively to the main peak at shorter wavelengths. As discussed earlier, under the 1PA mechanism the lower-energy band originates from the CT transitions, whereas the higher-energy peak corresponds to LC transitions. Namely, it appears that for **C1** and **4** the CT transitions promote the 2PA ability more effectively than LC transitions. Such an effect becomes even more pronounced with complex **C2**. An impressively large σ of 670 GM arises at a very long wavelength of 1040 nm as the overall 2PA maximum of **C2** (Figure 4). This 2PA peak approximately coincides with double the wavelength of the CT absorption band under linear excitation conditions. Such a 2PA σ value at >1000 nm is quite remarkable for transition-metal complexes. At a shorter wavelength of 740 nm, a shoulder peak of 120 GM is detected, corresponding to LC 2PA excitation of **C2**. However, such a phenomenon of CT-transition promoted 2PA does not occur universally to all complexes. In contrast to **C2**, metallacycle **C3** shows a 2PA maximum at 700 nm, corresponding to its LC transitions, whereas the 2PA activity related to CT transitions at longer wavelengths seems to be largely suppressed in this molecule (Figure 4).

DOI: 10.1021/am509074m
ACS Appl. Mater. Interfaces 2015, 7, 6162−6171

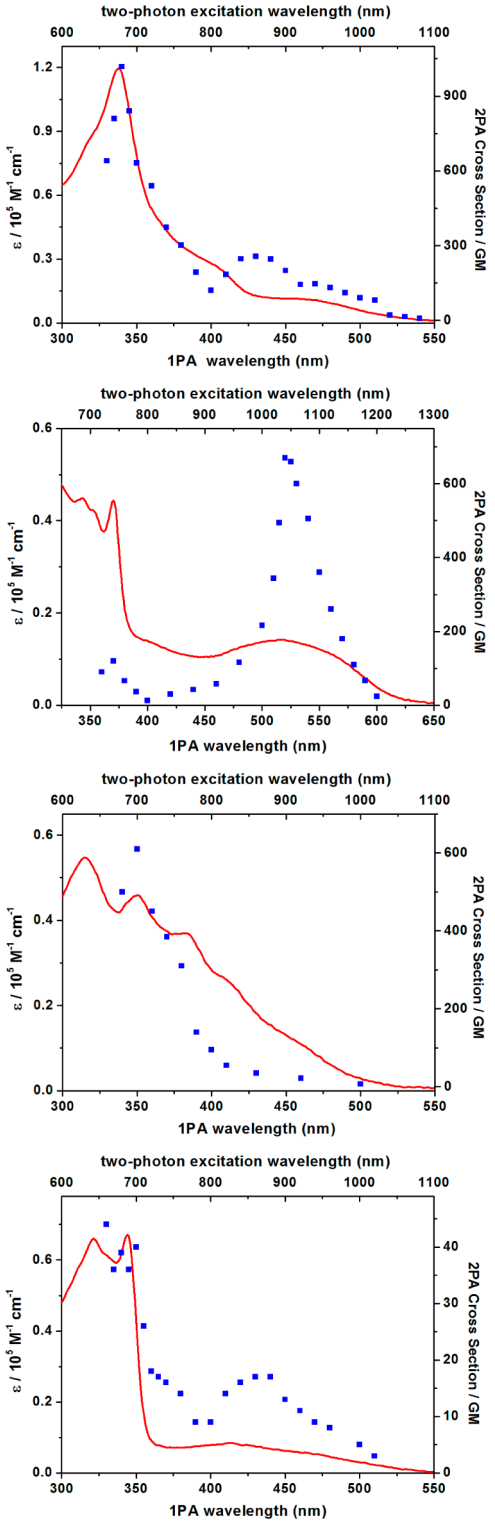

Figure 4. (blue ■) Two-photon absorption spectra in comparison to (red —) one-photon absorption spectra of (top to bottom) **C1**, **C2**, **C3**, and **4** in toluene.

We then compare the 2PA behaviors of **C1** in two different solvents, toluene and CH_2Cl_2. It is found that the two-photon excitation properties of **C1** in CH_2Cl_2 are very similar to those observed in toluene, except that the overall spectrum is slightly blue-shifted (Figure S19, Supporting Information). This shifting is similar in magnitude to that displayed by 1PA spectrum in response to the same solvent change. The 2PA properties in CH_2Cl_2 are also investigated for **C2** (Table 1). Again, a negative solvatochromic effect is detected for CT-related 2PA transitions, but minimal shifting is observed with LC two-photon excitation processes. Also, the 2PA maximum of **C2** displays a greater blue shift than **C1** upon solvent switching, from 1040 nm in toluene to 940 nm in CH_2Cl_2. This observation is also consistent with the 1PA behaviors. Basically, because consistent behaviors are exhibited by 1PA and two-photon excited emissions, it is implied that the two processes reach related excited states, and thus similar selection rules are applied.

Transient Absorption and Reverse Saturable Absorption. Subsequently, nanosecond transient difference absorption spectra are collected to characterize the triplet-state absorption properties of the complexes (Figures S20–S21 and Table S15, Supporting Information). Particularly, metallacycle **C1** in toluene exhibits prominent triplet excited-state absorptions in a broad range from 350 nm to over 800 nm (Figure 5). The

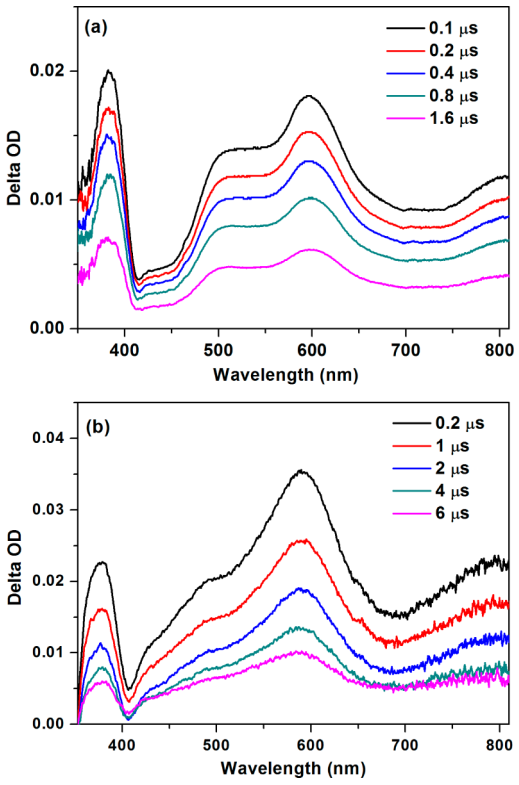

Figure 5. Nanosecond transient difference absorption spectra of **C1** at the specified delay times in (a) deoxygenated toluene and (b) CH_2Cl_2 (excited at 450 nm).

absorption peak around 380 nm is attributable to the phenanthroline anion radical,[28−32] reasonably resulting from ^{3}LLCT/MLCT excited state, while the broad band in the longer wavelength region can be assigned to the ^{3}LC state of the OPE ligand.[28] When the transient absorption spectrum is collected in CH_2Cl_2 solution, the absorption intensity around 380 nm is relatively decreased compared to that around 590 nm. The two bands both show monoexponential decays with identical lifetimes, but the decay rate is evidently slower in CH_2Cl_2 than toluene. These transient absorption results suggest that two types of triplet excited states (^{3}LLCT/MLCT vs ^{3}LC) are likely coexisting in dynamic equilibrium or admixed in **C1** at room temperature. The equilibrium position,

DOI: 10.1021/am509074m
ACS Appl. Mater. Interfaces 2015, 7, 6162−6171

or respective contribution, is dictated by the relative energy levels of the two states, which are sensitively influenced by the solvent polarity. For **C1** in toluene, because the ^{3}CT transition is of lower energy and possesses faster decay rates than ^{3}LC process, the former makes a great contribution and the complex relaxes faster. But the ^{3}CT energy gap is widened in more polar solvents such as CH_2Cl_2, the ^{3}LC transition thus becomes more prevalent and the decay rate decreases. These observations are consistent with the phosphorescence emission behaviors of the molecule.

As the transient absorption spectra show that **C1** presents intense triplet absorptions at over 500 nm, where its linear absorption is very weak, reverse saturate absorption (RSA) properties are examined with this molecule. To verify the RSA behaviors, we carried out open aperture Z-scan experiments[60] at 532 nm using ~10 ns (full-width half-maximum, fwhm) laser pulses. With an increasing laser power density, nonlinear absorption is clearly observed (Figure 6). Nonlinear transmission experiments are also conducted to further illustrate the RSA properties, which demonstrate that more pronounced RSA effect and larger excited-state vs ground-state absorption cross section ratios are shown by **C1** than **4** (Table S15 and Figure S23, Supporting Information). Such results further evidence the advantages of the designed metallacycles in NLO material developments.

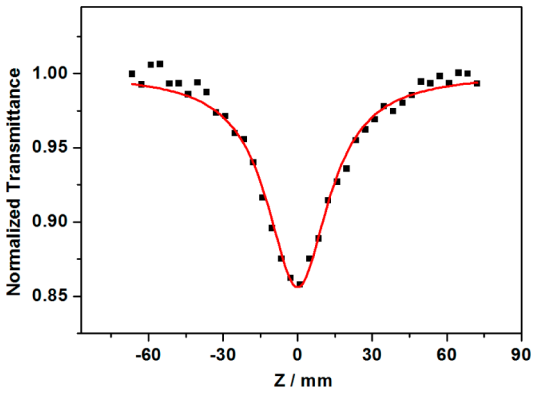

Figure 6. Normalized open-aperture data (black ■) of **C1** using 10 ns laser pulses at 532 nm and (red —) fitted curve.

CONCLUSIONS

In conclusion, we design and synthesize three platinum(II) diimine metallacycles incorporating large, cyclic conjugated bisacetylide ligands. Two types of triplet excited states, mainly featuring ^{3}LLCT/MLCT and ^{3}LC characteristics, respectively, may occur to these complexes depending on the size (conjugation length) and electronic features of the cyclic OPE ligands. Thus, their photophysical properties can be readily modulated by tailoring the OPE ligand structures. In one particular metallacycle, where the energy gaps of the ^{3}CT and ^{3}LC transitions are close to each other, the identity of the lowest triplet state is sensitively influenced by the solvent, as the two types of excited states undergo an energy inversion induced by the medium polarity change. DFT/TD-DFT calculations provide supportive evidence for such experimental conclusions. More importantly, the study shows that by virtue of the large, cyclic π-conjugated OPE ligand design, the metallacycles exhibit appealing NLO properties including pronounced two photon-excitation phosphorescence. By comparing them to an acyclic analogue, we demonstrated that the cyclic structural motif greatly improves the 2PA capacity. Among the three studied metallacycles, **C1** shows the largest 2PA cross section of 1020 GM at 680 nm, corresponding to the LC excitations, while **C2** manifests a considerable 2PA maximum around 1000 nm ($\sigma \approx 7 \times 10^2$ GM) related to CT excitations. These metallacycle structures also possess other useful NLO attributes, including broadband transient triplet-state absorptions and reverse saturable absorptions.

EXPERIMENTAL SECTION

Synthesis of C1. A Schlenk tube containing **L1** (90 mg, 0.087 mmol), Pt(phen)Cl_2 (39 mg, 0.087 mmol) and CuI (3.0 mg, 0.016 mmol) was evacuated and backfilled with nitrogen three times. Degassed toluene (100 mL) and diisopropylamine (20 mL) were added to the tube via a syringe under nitrogen atmosphere. The mixture was stirred at 90 °C for 72 h. Upon cooling to room temperature, the mixture was extracted with toluene. The organic layers were combined, washed with saturated aq NH_4Cl and dried over anhydrous Na_2SO_4 before the solvents were removed under reduced pressure. The crude product was purified with column chromatography and eluted with CH_2Cl_2 to offer **C1** as orange powder (32 mg, 26%). ^{1}H NMR ($CDCl_3$, 300 MHz, ppm): δ 9.91 (d, 2H, J = 4.2 Hz), 8.54 (d, 2H, J = 7.8 Hz), 7.93−7.88 (m, 4H), 7.61 (s, 4H), 7.53 (s, 8H), 7.04 (s, 2H), 7.02 (s, 2H), 4.05 (t, 8H, J = 6.3 Hz), 1.91−1.80 (m, 8H), 1.55−1.26 (m, 40H), 0.92−0.83 (m, 12H). ^{13}C NMR (100 MHz, $CDCl_3$, ppm): δ 151.6, 151.2, 149.9, 149.0, 147.9, 136.4, 132.5, 131.6, 130.3, 127.5, 126.5, 123.5, 122.3, 121.7, 121.5, 121.1, 116.5, 93.8, 92.9, 91.1, 90.4, 89.6, 89.1, 69.3, 69.2, 31.1, 29.4, 29.3, 29.2, 29.1, 26.3, 26.1, 22.9, 14.0. ESI-TOF HRMS: calcd, 1412.6783 ($[M + H]^+$); found, 1412.6832.

Synthesis of C2. Similar procedures for preparing **C1** were applied with **L2** as the substrate and dichloromethane (20 mL) as the solvent. The reaction mixture was stirred at 40 °C for 48 h. **C2** was obtained as a red solid (10 mg, 36%). ^{1}H NMR ($CDCl_3$, 300 MHz, ppm): δ 9.90 (d, 2H, J = 4.5 Hz), 8.10 (d, 2H, J = 7.8 Hz), 7.84 (m, 2H), 7.76 (s, 2H), 7.18 (s, 2H), 7.03 (s, 2H), 4.08 (m, 8H), 1.88 (m, 8H), 1.59−1.26 (m, 24H), 0.95 (m, 12H). ^{13}C NMR (100 MHz, $CDCl_3$, ppm): δ 151.5, 151.1, 147.8, 147.2, 136.4, 127.1, 121.3, 119.9, 117.6, 116.9, 115.3, 90.5, 89.6, 89.1, 69.5, 69.4, 31.6, 29.0, 25.6, 22.8, 14.1. ESI-TOF HRMS: calcd, 1022.4410 ($[M + Na]^+$); found, 1022.4418.

Synthesis of C3. Similar procedures for preparing **C1** were applied with **L3** as the substrate. The column chromatography was eluted with $CHCl_3$ to afford **3** as a yellow solid (12 mg, 32%). ^{1}H NMR ($CDCl_2CDCl_2$, 300 MHz, ppm): δ 9.97 (m, 2H), 8.69 (m, 2H), 8.06−8.00 (m, 8H), 7.73 (s, 4H), 7.65 (s, 8H), 3.70−3.65 (m, 4H), 1.92−1.84 (m, 4H), 1.62−1.21 (m, 20H), 0.92−0.85 (m, 6H). ESI-TOF HRMS: calcd, 1262.4184 ($[M + H]^+$); found, 1262.4152.

Synthesis of 4. A Schlenk tube containing **L4** (25 mg, 0.065 mmol), Pt(phen)Cl_2 (14 mg, 0.031 mmol), and CuI (3 mg, 0.016 mmol) was evacuated and backfilled with nitrogen three times. A mixture of degassed diisopropylamine (2.0 mL) and dichloromethane (14.0 mL) was added under nitrogen atmosphere. The reaction system was stirred at 40 °C for 40 h. Purification of the product was conducted with column chromatography, eluted with dichloromethane/petroleum ether (2:1, v/v), offering **4** as a yellow solid (29 mg, 74%). ^{1}H NMR ($CDCl_3$, 300 MHz, ppm): δ 9.91 (d, 2H, J = 5.1 Hz), 8.58 (d, 2H, J = 8.1 Hz), 7.95 (s, 2H), 7.88 (m, 2H), 7.50−7.36 (m, 12H), 6.86 (d, 4H, J = 8.1 Hz), 3.96 (t, 4H, J = 6.6 Hz), 1.83−1.74 (m, 4H), 1.55−1.26 (m, 36H), 0.89 (t, 6H, J = 6.6 Hz). ^{13}C NMR (100 MHz, $CDCl_3$, ppm): 159.2, 151.3, 147.7, 137.6, 132.9, 132.0, 130.9, 130.4, 128.1, 127.4, 125.9, 120.4, 115.6, 114.6, 90.1, 88.7, 68.2, 31.9, 29.6, 29.5, 29.4, 29.2, 26.1, 22.6, 14.1. ESI-TOF HRMS: calcd, 1146.5475 ($[M + H]^+$); found, 1146.5492.

Ground-State Photophysical Measurements. Ground-state UV−vis absorption spectra were recorded on a Hitachi U-4100 spectrophotometer in 1 cm quartz cuvettes. Steady-state photo-

DOI: 10.1021/am509074m
ACS Appl. Mater. Interfaces 2015, 7, 6162−6171

luminescence spectra were recorded on a Horiba Jobin Yvon FluoroMax-4P spectrofluorometer. Lifetime measurements were performed by time-correlated single-photon counting using a Horiba Jobin Yvon FluoroHub-B instrument, with NanoLED of 450 or 495 nm or pulsed xenon lamp as the excitation source. Sample solutions were deoxygenated by subjecting them to a minimum of three freeze−pump−thaw cycles before lifetime measurements or by bubbling through N_2 for 10 min before the emission quantum yield measurements. The absorbance of sample solutions used for emission quantum yield measurements was set to be between 0.05 and 0.1 at the excitation wavelength. $Ru(bpy)_3Cl_2$ was used as quantum yield standard (Φ_p = 0.062 in deoxygenated acetonitrile).[61]

Density Functional Theory Calculations. DFT and TD-DFT calculations were carried out using the Gaussian 09 suite of programs. The vibrational frequency calculations were conducted to ensure the optimized structures were the minimum on the potential energy surface. The structural geometry in the ground state (S_0) was optimized at the DFT level of theory without symmetry constraints. The geometry of the lowest triplet state (T_1) was optimized using an unrestricted formalism. For each complex, 50 singlet and 6 triplet excited states were obtained to determine the vertical excitation energies on the basis of optimized geometrical structures.

Nonlinear Optical Measurements. A femtosecond laser system composed of a Spectra-Physics TOPAS optical parametric amplifier (OPA) pumped by a Spfire ACE-F-1KXP Ti:sapphire amplifier (~120 fs, 1 kHz) was used for two-photon excitation phosphorescence experiments. The short pulse duration and low repetition rate ensure accurate 2PA cross-sectional measurements with minimum excited-state absorption and cumulative effects of consecutive pulses. The OPA had signal and idler wavelength tuning ranges of 1100−1600 and 1600−2600 nm, respectively. To obtain varied wavelengths in the range of 650−1200 nm, the second harmonic of the signal or idler was used in the 650−800 or 800−1100 nm regions, and the signal wavelength was used at 1100−1200 nm. The pulse from OPA was focused by a lens with a focal length of 50 cm. To minimize the effects of reabsorption, the excitation beam was moved as close as possible to the wall of the quartz cell facing the slit of the imaging spectrograph. The emission was detected in the direction perpendicular to the pump beam. Two-photon cross sections were determined by comparative measurements using Rhodamine B in methanol as the reference.[59]

Nanosecond transient absorption measurements were performed on an LP-920 laser flash photolysis setup (Edinburgh). Excitation light of 450 nm from a computer-controlled Nd:YAG laser/OPO system from Opotek (Vibrant 355 II) operating at 10 Hz was directed to the samples. The open aperture Z-scan and corresponding nonlinear transmission experiments were carried out with toluene solutions in 1 mm cuvettes using ~10 ns laser pulses. A homemade ns optical parametric oscillator (OPO) laser with a repetition rate of 10 Hz was used as the light source. The spatial profile of the laser beam was a nearly Gaussian distribution. The beam was focused by plano-convex lens with a focal length of 200 mm. By fitting the open aperture Z-scan data, the excited-state absorption cross section (σ_{ex}) was obtained.

■ ASSOCIATED CONTENT

Supporting Information

Additional synthesis procedures, photophysical characterizations, and computational results. This material is available free of charge via the Internet at http://pubs.acs.org.

■ AUTHOR INFORMATION

Corresponding Author

*E-mail: dhzhao@pku.edu.cn.

Notes

The authors declare no competing financial interest.

■ ACKNOWLEDGMENTS

This work was supported by the National Natural Science Foundation of China (No. 21174004, 21222403 and 51473003).

■ REFERENCES

(1) Cheng, G.; Kui, S. C. F.; Ang, W.-H.; Ko, M.-Y.; Chow, P.-K.; Kwong, C.-L.; Kwok, C.-C.; Ma, C.; Guan, X.; Low, K.-H.; Su, S.-J.; Che, C.-M. Structurally Robust Phosphorescent [Pt(O∧N∧C∧N)] Emitters for High Performance Organic Light-Emitting Devices with Power Efficiency up to 126 lm W^{-1} and External Quantum Efficiency over 20%. *Chem. Sci.* **2014**, *5*, 4819−4830.

(2) Lu, W.; Mi, B.-X.; Chan, M. C. W.; Hui, Z.; Che, C.-M.; Zhu, N.; Lee, S.-T. Light-Emitting Tridentate Cyclometalated Platinum(II) Complexes Containing σ-Alkynyl Auxiliaries: Tuning of Photo- and Electrophosphorescence. *J. Am. Chem. Soc.* **2004**, *126*, 4958−4971.

(3) Wong, W.-W.; Ho, C.-L. Organometallic Photovoltaics: A New and Versatile Approach for Harvesting Solar Energy Using Conjugated Polymetallaynes. *Acc. Chem. Res.* **2010**, *43*, 1246−1256.

(4) Chung, C. Y.-S.; Li, S. P.-Y.; Louie, M.-W.; Lo, K. K.-W.; Yam, V. W.-W. Induced Self-Assembly and Disassembly of Water-Soluble Alkynylplatinum(II) Terpyridyl Complexes with "Switchable" Near-Infrared (NIR) Emission Modulated by Metal-Metal Interactions over Physiological pH: Demonstration of pH-Responsive NIR Luminescent Probes in Cell-Imaging Studies. *Chem. Sci.* **2013**, *4*, 2453−2462.

(5) Ni, J.; Zhang, X.; Wu, Y.-H.; Zhang, L.-Y.; Chen, Z.-N. Vapor- and Mechanical-Grinding-Triggered Color and Luminescence Switches for Bis(*s*-fluorophenylacetylide) Platinum(II) Complexes. *Chem.—Eur. J.* **2011**, *17*, 1171−1183.

(6) Yam, V. W.-W.; Chan, K. H.-Y.; Wong, K. M.-C.; Zhu, N. Luminescent Platinum(II) Terpyridyl Complexes: Effect of Counter Ions on Solvent-Induced Aggregation and Color Changes. *Chem.—Eur. J.* **2005**, *11*, 4535−4543.

(7) Zhao, J.; Ji, S.; Wu, W.; Wu, W.; Guo, H.; Sun, J.; Sun, H.; Liu, Y.; Li, Q.; Huang, L. Transition Metal Complexes with Strong Absorption of Visible Light and Long-Lived Triplet Excited States: From Molecular Design to Applications. *RSC Adv.* **2012**, *2*, 1712−1728.

(8) Wu, W.; Zhao, J.; Sun, J.; Huang, L.; Yi, X. Red-Light Excitable Fluorescent Platinum(II) Bis(aryleneethynylene) Bis-(trialkylphosphine) Complexes Showing Long-Lived Triplet Excited States as Triplet Photosensitizers for Triplet−Triplet Annihilation Upconversion. *J. Mater. Chem.C* **2013**, *1*, 705−716.

(9) Williams, J. A. G. Photochemistry and Photophysics of Coordination Compounds: Platinum. *Top. Curr. Chem.* **2007**, *281*, 205−268.

(10) Muro, M. L.; Rachford, A. A.; Wang, X.; Castellano, F. N. Platinum^{II} Acetylide Photophysics. *Top. Organmet. Chem.* **2010**, *29*, 159−191.

(11) Yam, V. W.-W.; Wong, K. M.-C. Luminescent Metal Complexes of d^6, d^8, and d^{10} Transition Metal Centres. *Chem. Commun.* **2011**, *47*, 11579−11592.

(12) Wong, K. M.-C.; Yam, V. W.-W. Self-Assembly of Luminescent Alkynylplatinum(II) Terpyridyl Complexes: Modulation of Photophysical Properties through Aggregation Behavior. *Acc. Chem. Res.* **2011**, *44*, 424−434.

(13) He, G. S.; Tan, L.-S.; Zheng, Q.; Prasad, P. N. Multiphoton Absorbing Materials: Molecular Designs, Characterizations, and Applications. *Chem. Rev.* **2008**, *108*, 1245−1330.

(14) Pawlicki, M.; Collins, H. A.; Denning, R. G.; Anderson, H. L. Two-Photon Absorption and the Design of Two-Photon Dyes. *Angew. Chem., Int. Ed.* **2009**, *48*, 3244−3266.

(15) Marder, S. R. Organic Nonlinear Optical Materials: Where We Have Been and Where We Are Going. *Chem. Commun.* **2006**, 131−134.

(16) Li, L.; Fourkas, J. T. Multiphoton Polymerization. *Mater. Today* **2007**, *10*, 30−37.

DOI: 10.1021/am509074m
ACS Appl. Mater. Interfaces 2015, 7, 6162−6171

(17) Belfield, K. D.; Yao, S.; Bondar, M. V. Two-Photon Absorbing Photonic Materials: From Fundamentals to Applications. *Adv. Polym. Sci.* **2008**, *213*, 97−156.
(18) Zhou, G.-J.; Wong, W.-W. Organometallic Acetylides of Pt^{II}, Au^{I} and Hg^{II} as New Generation Optical Power Limiting Materials. *Chem. Soc. Rev.* **2011**, *40*, 2541−2566.
(19) Liao, C.; Shelton, A. H.; Kim, K.-Y.; Schanze, K. S. Organoplatinum Chromophores for Application in High-Performance Nonlinear Absorption Materials. *ACS Appl. Mater. Interfaces* **2011**, *3*, 3225−3238.
(20) Rogers, J. E.; Slagle, J. E.; Krein, D. M.; Burke, A. R.; Hall, B. C.; Fratini, A.; McLean, D. G.; Fleitz, P. A.; Cooper, T. M.; Drobizhev, M.; Makarov, N. S.; Rebane, A.; Kim, K.-Y.; Farley, R.; Schanze, K. S. Platinum Acetylide Two-Photon Chromophores. *Inorg. Chem.* **2007**, *46*, 6483−6494.
(21) Liu, R.; Azenkeng, A.; Zhou, D.; Li, Y.; Glusac, K. D.; Sun, W. Tuning Photophysical Properties and Improving Nonlinear Absorption of Pt(II) Diimine Complexes with Extended π-Conjugation in the Acetylide Ligands. *J. Phys. Chem. A* **2013**, *117*, 1907−1917.
(22) Melekhova, A. A.; Krupenya, D. V.; Gurzhiy, V. V.; Melnikov, A. S.; Serdobintesv, P. Y.; Selivanov, S. I.; Tunik, S. P. Synthesis, Characterization, Luminescence and Non-Linear Optical Properties of Diimine Platinum(II) Complexes with Arylacetylene Ligands. *J. Organomet. Chem.* **2014**, *763*, 1−5.
(23) Glimsdal, E.; Carlsson, M.; Eliasson, B.; Minaev, B.; Lindgren, M. Excited States and Two-Photon Absorption of Some Novel Thiophenyl Pt(II)−Ethynyl Derivatives. *J. Phys. Chem. A* **2007**, *111*, 244−250.
(24) Samoc, M.; Dalton, G. T.; Gladysz, J. A.; Zheng, Q.; Velkov, Y.; Ågren, H.; Norman, P.; Humphrey, M. G. Cubic Nonlinear Optical Properties of Platinum-Terminated Polyynediyl Chains. *Inorg. Chem.* **2008**, *47*, 9946−9957.
(25) Kim, K.-Y.; Shelton, A. H.; Drobizhev, M.; Makarov, N.; Rebane, A.; Schanze, K. S. Optimizing Simultaneous Two-Photon Absorption and Transient Triplet-Triplet Absorption in Platinum Acetylide Chromophores. *J. Phys. Chem. A* **2010**, *114*, 7003−7013.
(26) Goudreault, T.; He, Z.; Guo, Y.; Ho, C.-L.; Zhan, H.; Wang, Q.; Ho, K. Y.-F.; Wong, K.-L.; Fortin, D.; Yao, B.; Xie, Z.; Wang, L.; Kwok, W.-M.; Harvey, P. D.; Wong, W.-Y. Synthesis, Light-Emitting, and Two-Photon Absorption Properties of Platinum-Containing Poly(arylene-ethynylene)s Linked by 1,3,4-Oxadiazole Units. *Macromolecules* **2010**, *43*, 7936−7949.
(27) Dubinina, G. G.; Price, R. S.; Abboud, K. A.; Wicks, G.; Wnuk, P.; Stepanenko, Y.; Drobizhev, M.; Rebane, A.; Schanze, K. S. Phenylene Vinylene Platinum(II) Acetylides with Prodigious Two-Photon Absorption. *J. Am. Chem. Soc.* **2012**, *134*, 19346−10349.
(28) Pomestchenko, I. E.; Castellano, F. N. Solvent Switching between Charge Transfer and Intraligand Excited States in a Multichromophoric Platinum(II) Complex. *J. Phys. Chem. A* **2004**, *108*, 3485−3492.
(29) Geob, S.; Rachford, A. A.; Castellano, F. N. Solvent-Induced Configuration Mixing and Triplet Excited State Inversion Exemplified in A Pt(II) Complex. *Chem. Commun.* **2008**, 814−816.
(30) Sun, W.; Zhang, B.; Li, Y.; Pritchett, T. M.; Li, Z.; Haley, J. E. Broadband Nonlinear Absorbing Platinum 2,2′-Bipyridine Complex Bearing 2-(Benzothiazol-2′-yl)-9,9-diethyl-7-ethynylfluorene Ligands. *Chem. Mater.* **2010**, *22*, 6384−6392.
(31) Whittle, C. E.; Weinstein, J. A.; George, M. W.; Schanze, K. S. Photophysics of Diimine Platinum(II) Bis-Acetylide Complexes. *Inorg. Chem.* **2001**, *40*, 4053−4062.
(32) Danilov, E. O.; Pomestchenko, I. E.; Kinayyigit, S.; Gentili, P. L.; Hissler, M.; Ziessel, R.; Castellano, F. N. Ultrafast Energy Migration in Platinum(II) Diimine Complexes Bearing Pyrenylacetylide Chromophores. *J. Phys. Chem. A* **2005**, *109*, 2465−2471.
(33) Rachford, A. A.; Goeb, S.; Ziessel, R.; Castellano, F. N. Ligand Localized Triplet Excited States in Platinum(II) Bipyridyl and Terpyridyl Peryleneacetylides. *Inorg. Chem.* **2008**, *47*, 4348−4355.
(34) Hua, F.; Kinayyigit, S.; Cable, J. R.; Castellano, F. N. Platinum(II) Diimine Diacetylides: Metallacyclization Enhances Photophysical Properties. *Inorg. Chem.* **2006**, *45*, 4304−4306.
(35) Li, R.; Azenkeng, A.; Li, Y.; Sun, W. Long-Lived Platinum(II) Diimine Complexes with Broadband Excited-State Absorption: Efficient Nonlinear Absorbing Materials. *Dalton Trans.* **2012**, *41*, 12353−12357.
(36) Liu, R.; Dandu, N.; Li, Y.; Kilina, S.; Sun, W. Synthesis, Photophysics, and Reverse Saturable Absorption of Bipyridyl Platinum(II) Bis(arylfl uorenylacetylide) Complexes. *Dalton Trans.* **2013**, *42*, 4398−4409.
(37) Liu, R.; Chen, H.; Chang, J.; Li, Y.; Zhu, H.; Sun, W. Pt(II) Diimine Complexes Bearing Carbazolyl-Capped Acetylide Ligands: Synthesis, Tunable Photophysics and Nonlinear Absorption. *Dalton Trans.* **2013**, *42*, 160−171.
(38) Li, Y.; Liu, R.; Badaeva, E.; Kilina, S.; Sun, W. Long-Lived π-Shape Platinum(II) Diimine Complexes Bearing 7-Benzothiazolyl-fluoren-2-yl Motif on the Bipyridine and Acetylide Ligands: Admixing π,π^* and Charge-Transfer Configurations. *J. Phys. Chem. C* **2013**, *117*, 5908−5918.
(39) Li, Y.; Wu, W.; Zhao, J.; Zhang, X.; Guo, H. Accessing the Long-Lived Near-IR-Emissive Triplet Excited State in Naphthalenediimide with Light-Harvesting Diimine Platinum(II) Bisacetylide Complex and Its Application for Upconversion. *Dalton Trans.* **2011**, *40*, 9085−9089.
(40) Sun, H.; Guo, H.; Wu, W.; Liu, X.; Zhao, J. Coumarin Phosphorescence Observed with N[∧]NPt(II) Bisacetylide Complex and Its Applications for Luminescent Oxygen Sensing and Triplet−Triplet-Annihilation Based Upconversion. *Dalton Trans.* **2011**, *40*, 7834−7841.
(41) Huang, L.; Zeng, L.; Guo, H.; Wu, W.; Wu, W.; Ji, S.; Zhao, J. Room-Temperature Long-Lived ^{3}IL Excited State of Rhodamine in an *NN* Pt^{II} Bis(acetylide) Complex with Intense Visible-Light Absorption. *Eur. J. Inorg. Chem.* **2011**, 4527−4533.
(42) Ahn, T. K.; Kim, K. S.; Kim, D. Y.; Noh, S. B.; Aratani, N.; Ikeda, C.; Osuka, A.; Kim, D. Relationship between Two-Photon Absorption and the π-Conjugation Pathway in Porphyrin Arrays through Dihedral Angle Control. *J. Am. Chem. Soc.* **2006**, *128*, 1700−1704.
(43) Hisaki, I.; Hiroto, S.; Kim, K. S.; Noh, S. B.; Kim, D.; Shinokubo, H.; Osuka, A. Synthesis of Doubly β-to-β 1,3-Butadiyne-Bridged Diporphyrins: Enforced Planar Structures and Large Two-Photon Absorption Cross Sections. *Angew. Chem., Int. Ed.* **2007**, *46*, 5125−5128.
(44) Williams-Harry, M.; Bhaskar, A.; Ramakrishna, G.; Goodson, T.; Imamura, M.; Mawatari, A.; Nakao, K.; Enozawa, H.; Nishinaga, T.; Iyoda, M. Giant Thienylene-Acetylene-Ethylene Macrocycles with Large Two-Photon Absorption Cross Section and Semishape-Persistence. *J. Am. Chem. Soc.* **2008**, *130*, 3252−3253.
(45) Blanco, V.; García, M. D.; Terenzi, A.; Pía, E.; Fernéndez-Mato, A.; Peinador, C.; Quintela, J. M. Complexation and Extraction of PAHs to the Aqueous Phase with a Dinuclear Pt^{II} Diazapyrenium-Based Metallacycle. *Chem.—Eur. J.* **2010**, *16*, 12373−12380.
(46) López-Vidal, E. M.; Blanco, V.; García, M. D.; Peinador, C.; Quintela, J. M. Synthesis of Platinum(II) Metallocycles Using Microwave-Assisted Heating. *Org. Lett.* **2012**, *14*, 580−583.
(47) Pollock, J. B.; Cook, T. R.; Stang, P. J. Photophysical and Computational Investigations of Bis(phosphine) Organoplatinum(II) Metallacycles. *J. Am. Chem. Soc.* **2012**, *134*, 10607−10620.
(48) Pollock, J. B.; Schneider, G. L.; Cook, T. R.; Davis, A. S.; Stang, P. J. Tunable Visible Light Emission of Self-Assembled Rhomboidal Metallacycles. *J. Am. Chem. Soc.* **2013**, *135*, 13676−13679.
(49) Chen, J.-S.; Zhao, G.-J.; Cook, T. R.; Han, K.-L.; Stang, P. J. Photophysical Properties of Self-Assembled Multinuclear Platinum Metallacycles with Different Conformational Geometries. *J. Am. Chem. Soc.* **2013**, *135*, 6694−6702.
(50) Luo, J.; Yan, Q.; Zhou, Y.; Li, T.; Zhu, N.; Bai, C.; Cao, Y.; Wang, J.; Pei, J.; Zhao, D. A Photoswitch Based on Self-Assembled Single Microwire of A Phenyleneethynylene Macrocycle. *Chem. Commun.* **2010**, *46*, 5725−5727.

DOI: 10.1021/am509074m
ACS Appl. Mater. Interfaces 2015, 7, 6162−6171

(51) Chan, C. W.; Chen, L. K.; Che, C. M. Structures and Photoluminescence of Dinuclear Platinum(II) and Palladium(II) Complexes with Bridging Thiolates and 2,2′-Bipyridine or 2,2′:6′,2″-Terpyridine Ligands. *Coord. Chem. Rev.* **1994**, *132*, 87−97.
(52) Hissler, M.; Connick, W. B.; Geiger, D. K.; McGarrah, J. E.; Lipa, D.; Lachicotte, R. J.; Eisenberg, R. Platinum Diimine Bis(acetylide) Complexes: Synthesis, Characterization, and Luminescence Properties. *Inorg. Chem.* **2000**, *39*, 447−457.
(53) McGarrah, J. E.; Eisenberg, R. Dyads for Photoinduced Charge Separation Based on Platinum Diimine Bis(acetylide) Chromophores: Synthesis, Luminescence, and Transient Absorption Studies. *Inorg. Chem.* **2003**, *42*, 4355−4365.
(54) Guo, H.; Muro-Small, M. L.; Ji, S.; Zhao, J.; Castellano, F. N. Naphthalimide Phosphorescence Finally Exposed in a Platinum(II) Diimine Complex. *Inorg. Chem.* **2010**, *49*, 6802−6804.
(55) Hua, F.; Kinayyigit, S.; Rachford, A. A.; Shikhova, E. A.; Goeb, S.; Cable, J. R.; Adams, C. J.; Kirschbaum, K.; Pinkerton, A. A.; Castellano, F. N. Luminescent Charge-Transfer Platinum(II) Metallacycle. *Inorg. Chem.* **2007**, *46*, 8771−8783.
(56) Frisch, M. J.; et al. *Gaussian 09*, revision C.1; Gaussian, Inc.: Wallingford, CT, 2010.
(57) Zhang, B.; Li, Y.; Liu, R.; Pritchett, T. M.; Haley, J. E.; Sun, W. Extending the Bandwidth of Reverse Saturable Absorption in Platinum Complexes Using Two-Photon-Initiated Excited-State Absorption. *ACS Appl. Mater. Interfaces* **2013**, *5*, 565−572.
(58) Koo, C.-K.; Wong, K.-L.; Man, C. W.-Y.; Tam, H.-L.; Tsao, S.-W.; Cheah, K.-W.; Lam, H.-W. Two-Photon Plasma Membrane Imaging in Live Cells by an Amphiphilic, Water-Soluble Cyctometalated Platinum(II) Complex. *Inorg. Chem.* **2009**, *48*, 7501−7503.
(59) Makarov, N. S.; Drobizhev, M.; Rebane, A. Two-Photon Absorption Standards in the 550−1600 nm Excitation Wavelength Range. *Opt. Express* **2008**, *16*, 4029−4047.
(60) Sheik-Bahae, M.; Said, A. A.; Wei, T.-H.; Hagan, D. J.; Van Stryland, E. W. Sensitive Measurement of Optical Nonlinearities Using a Single Beam. *IEEE J. Quantum Electron.* **1990**, *26*, 760−769.
(61) Lowry, M. S.; Hudson, W. R.; Pascal, R. A.; Bernhard, S. Accelerated Luminophore Discovery through Combinatorial Synthesis. *J. Am. Chem. Soc.* **2004**, *126*, 14129−14135.

DOI: 10.1021/am509074m
ACS Appl. Mater. Interfaces 2015, 7, 6162−6171